**ORIGINAL ARTICLE**

# CREB1 Silencing Protects Against Inflammatory Response in Rats with Deep Vein Thrombosis Through Reducing RPL9 Expression and Blocking NF-κB Signaling

Xiaorong Jian[1] · Dehua Yang[2] · Li Wang[1] · Hongxiang Wang[1]

## Abstract

Apoptosis and inflammation of vascular endothelial cells (VECs) are the most important causes of deep vein thrombosis (DVT). cAMP response element binding protein 1 (CREB1) encodes a transcription factor that binds as a homodimer to the cAMP-responsive element and can promote inflammation. CREB1 is found to be upregulated in the plasma of patients with venous thromboembolism. However, the biological functions of CREB1 in DVT remain unknown. We evaluated the effect of CREB1 in a rat model of inferior vena cava (IVA) stenosis-induced DVT. IVC stenosis resulted in stable thrombus, inflammatory response and CREB1 upregulation, whereas CREB1 knockdown inhibited thrombus and inflammation in DVT rats. In vitro analysis showed that CREB1 knockdown inhibited VEC apoptosis. Mechanistically, CREB1 knockdown reduced Ribosomal protein L9 (RPL9) expression and blocked the NF-κB pathway. Therefore, CREB1 may become a potential therapeutic target of DVT prevention.

**Keywords** Deep vein thrombosis · CREB1 · Inferior vena cava · Inflammation · RPL9 · NF-κB

## Introduction

Deep vein thrombosis (DVT) is a postsurgical complication of lower limb fracture that affects approximately 250,000 patients every year [1, 2]. DVT can lead to pulmonary hypertension, fatal pulmonary embolism, repeated thrombosis, and post-thrombotic syndrome [3, 4]. Surgical treatment is a widely accepted therapeutic option, but vascular endothelial cells (VECs) may be destroyed post-surgery, thereby leading to an increase in the risk of thrombosis recurrence and poor prognosis [5]. Additionally, warfarin, heparin, aspirin, and clopidogrel are regarded as effective anticoagulants for DVT prevention. However, these anticoagulants are associated with high risk of major bleeding [6]. Thus, better understanding the underlying mechanisms and exploring novel biomarkers are necessary for the diagnosis, prevention and prognosis of DVT.

In addition to blood coagulation, fibrinolysis, and thickness regarded as the main pathogenesis, recent evidence has suggested that inflammation also plays an important role in thrombosis [7–9]. As reported, infiltration of neutrophils, monocytes, and lymphocytes in the vein wall is recognized as a key event during DVT process [10]. Neutrophils account for over 80% of inflammatory cells, and the neutrophil extracellular traps released from neutrophils can activate coagulation [11]. Active monocytes can secret inflammatory cytokines [10, 12]. Intriguingly, nuclear factor-kappa B (NF-κB) is regarded as an important transcription factor in inflammatory response and can modular above-mentioned molecules [13]. Higher NF-κB level is observed in DVT patients than those in healthy controls and patients without DVT after surgery [14]. Accumulation of inflammatory factors into venous thrombus and

---

Associate Editor Junjie Xiao oversaw the review of this article

Xiaorong Jian and Dehua Yang contributed equally to this work.

✉ Xiaorong Jian
  xiaorongjane@126.com

✉ Hongxiang Wang
  whitely1972@sina.com

1 Department of Hematology, The Central Hospital of Wuhan, Tongji Medical College, Huazhong University of Science and Technology, No. 26, Shengli Street, Jiang'an District, Wuhan 430014, Hubei, China

2 Department of Pediatric Surgery, Union Hospital, Tongji Medical College, Huazhong University of Science and Technology, Wuhan 430022, China

vein wall is prevented through inhibition of NF-κB signaling [15]. Collectively, inhibition of NF-κB-mediated inflammatory responses is beneficial to alleviate DVT.

Transcription factors (TFs) are suggested to regulate gene expression through binding to the promoter region of target genes, and are identified to regulate various pathophysiologic processes, including cardiovascular diseases and VTE [16]. For example, hypoxia-inducible factor-1 alpha (HIF1α), a TF targeting vascular endothelial growth factor (VEGF), has been shown to promote angiogenesis and accelerate thrombus resolution and vein recanalization in experimental DVT model [17, 18]. Additionally, Wang et al. articulate that Yin Yang 1 (YY1) upregulates vitronectin expression by binding to its promoter region and decreased their binding efficiency can increase the risk of DVT [19]. CAMP-response element-binding protein 1 (CREB1) encodes a transcription factor that binds as a homodimer to the cAMP-responsive element. The phosphorylated status of CREB1 can induce gene transcription to respond to hormonal stimulation of the cAMP pathway [20]. CREB can drive thrombospondin-1 transcription and regulate the formation and maintenance of arterial thrombosis [21, 22]. A previous study has postulated that CREB1 may play a critical role in venous thromboembolism (VTE) and endothelial cell metabolism [23]. Analysis of TFs-regulatory network of differentially expressed genes in VTE shows that CREB1 regulate the expression of ribosomal protein L9 (RPL9) that is highly expressed in VTE samples [24]. However, the biological functions of CREB1 and whether CREB1 transcriptionally regulates RPL9 expression in DVT remain uncertain. Some studies have suggested that CREB1 and RPL9 knockdown can inactivate the NF-κB pathway [25–27]. Thus, this study is performed to explore the biological functions of CREB1 in inflammation of DVT rats and the potential mechanism in relation to RPL9 and NF-κB signaling.

# Methods

## Animals

Sprague–Dawley (SD) rats (male, 8–12 weeks of age, 200–300 g; SJA Laboratory Animal CO., LTD, Hunan, China) were housed in a room with controlled temperature of $24 \pm 0.5°C$ and $55 \pm 5\%$ humidity under a 12-h light/dark cycle. All rats were given free access to food and water. All experiments involving animals were approved by the Animal Ethics Committee of Hospital, and all experimental protocols strictly followed the Guide for the Care and Use of Laboratory Animals published by the National Institutes of Health (NIH publication no.85–23, revised 1996).

## Establishment of Experimental DVT

Thrombosis was induced by inferior vena cava (IVC) stenosis as previously described [28]. Briefly, the rats were given 7 days to acclimate and then fasted for 12 h. Subsequently, the rats were anesthetized with intraperitoneal injection of 1% pentobarbital sodium (40 mg/kg; Sigma-Aldrich, Shanghai, China) and immobilized on the operating table at a supine position. Next, a 2-cm incision was made along the abdominal midline, and the IVC was disserted and exposed. Thereafter, the IVC was stenosed by putting a 20 G needle (diameter: 0.91 mm) outside the vein, trying with a 7–0 silk at about 1 mm below the left renal vein, and removing the needle. After surgery, the abdominal muscle and skin were sutured, and ceftriaxone sodium (TopScience, Shanghai, China) was sprinkled evenly along the incision to prevent bacterial infection. Sham operation included the same surgical procedure without IVC stenosis.

## Transfection with siRNA

Adenoviral constructs carrying siRNA against CREB1 were designed and produced by GenePharma (Shanghai, China). The siRNA sequences were inserted into the pAdeno-U6-EGFP vector, and recombinant siRNA plasmids were transfected into HEK293T cells (Procell, Wuhan, China). The siRNA targeted sequences of CREB1 were 5'-GGAGTCTGTGGATAGTGTA-3'. The siRNA targeted sequences of negative control (si-NC) were 5'TTCTCCGAACGTGTCACGT-3'.

## Animal Groups

The current study totally recruited 50 rats. Among these animals, rat VECs were isolated from 10 rats with IVC-stenosed DVT. The remaining rats were classified into four groups: (a) the sham group, the rats received sham operation; (b) the Model group, the rats underwent IVC stenosis; (c) the Model + si-NC group, the rats were injected with 20 ml transfection compound containing 400 pmol of si-NC through the tail vein; (d) the Model + si-CREB1 group, the rats were injected with 20 ml transfection compound containing 400 pmol of CREB1 siRNA. Each group had 10 rats.

## Sample Collection

The animals were intraperitoneally injected with 1% pentobarbital sodium after 24 h of injection and venous plasma was harvested from the IVC using a vacuum blood tube without anticoagulants followed by immediate shocking. Thereafter, the rats were euthanized by decapitation after

deep anesthesia. Afterwards, the thrombus-containing IVC was carefully removed for weight assessment. The IVCs were split into two parts after clearing unclotted blood: one was fixed with 4% paraformaldehyde for histopathologic analysis and the other was stored at -80℃ for western blotting, RT-qPCR, and immunofluorescence analyses.

## Histological Analysis

The 4% paraformaldehyde-fixed IVCs were subjected to degradation through graded alcohol, and then embedded in paraffin and sectioned into 4-μm slices. Next, the slices were processed for 15-min hematoxylin staining (Solarbio, Beijing, China), differentiated for 30 s, and soaked for 5 min at 50℃. Thereafter, the sections were stained with eosin (Solarbio) for 40 s followed by washing using phosphate buffered saline (PBS), dehydration, and clearing via xylene (Solarbio). Finally, the slices were observed under a light microscope (Olympus, Tokyo, Japan). The thrombosis was assessed and recorded by pathological professionals according to the histological examination of thrombus grading evaluation criteria. If the thrombosis was uncertain, the proximal, middle and distal points were obtained for slicing and the points with obvious thrombus were included in the statistics. According to the degree of vascular obstruction by thrombus, 0 represented no thrombus, 1 represented vascular obstruction < 50%, 2 represented vascular obstruction > 50% (not completely blocked), and 3 represented complete vascular obstruction [29].

## Isolation and Treatment of Rat VECs

The rats were anesthetized by intraperitoneal injection of 1% pentobarbital sodium, and soaked for 10 min in 75% ethanol. Then, the abdominal cavity was exposed under sterile conditions, and approximately 3 mL of cord blood was collected with anticoagulant treatment by heparin, mixed with PBS at a 1:1 ratio, mixed with 0.5% methyl cellulose (MedChemExpress, Shanghai, China) at 4:1 ratio, and placed at room temperature for 30 min for erythrocyte sedimentation. The supernatant was added to a rat lymphocyte isolation with a density of 1.803 g/mL and centrifuged for 20 min with a centrifugal radius of 18.5 cm, 1200 rpm. The boundary layer was resuspended by adding PBS and centrifuging 8 min with a centrifugal radius of 18.5 cm, 800 rpm, and washed with PBS. To the pellet, 5-mL VEC induction medium (Dulbecco's modified Eagle medium supplemented with 10% fetal bovine serum, 1% penicillin, 1% streptomycin, 20 μg/L VEGF, 2 μg/L IGF-1, 2 μg/L bFGF and 20 μg/L EGF). The cell suspension was placed in 25 cm$^2$ culture flasks and incubated at 37℃, 5% $CO_2$ and saturated humidity. When primary cells fused and covered 90% of the bottom of the flask, 0.25% trypsin and 0.01% EDTA (Sigma-Aldrich) were added, and the cells were subcultured at a 1:2 ratio.

The VECs were seeded onto 6-well plates, and when reaching 80% confluence, the cells were introduced with si-NC, si-CREB1, and combination of si-CREB1 and pcDNA3.1-RPL9 using Lipofectamine 2000 (Sigma-Aldrich) and harvested after 48 h of transfection. These plasmids were obtained from GenePharma. To repress the activation of NF-κB, the cells were pretreated with 40 nM 4-N-[2-(4-phenoxyphenyl) ethyl] quinazoline-4,6-diamine (QNZ; MedChemExpress) 1 h after si-CREB1 and pcDNA3.1-RPL9 intervention.

## Reverse Transcription Quantitative Real-time Polymerase Chain Reaction (RT-qPCR)

Total RNA was isolated from frozen IVCs and transfected VECs using the TRIzol solution (Beyotime, Shanghai, China), and the RNA purity was determined by spectrophotometer (Thermo Fisher Scientific, Waltham, MA, USA). Primers were designed and synthesized by Takara (Otsu, Shiga, Japan). Subsequently, RNA was reverse transcribed into cDNA through using PrimeScript RT kit (TaKaRa). The relative level of mRNA was determined using a SYBR Green real-time PCR Kit (Solarbio). The qPCR thermocycling conditions were 95℃ for 1 min followed by 40 cycles of 95℃ for 10 s, and 60℃ for 34 s, and a final extension at 60℃ for 1 min. RT-qPCR was performed using ABI7500 system (Thermo Fisher Scientific). GAPDH was used as an internal reference. Relative quantification was conducted via the $2^{-\Delta\Delta Cq}$ method [30]. The primer sequences were listed in Table 1.

## Western Blotting

The frozen IVCs and treated VECs were lysed using RIPA buffer (Sigma-Aldrich) containing protease inhibitor (ApexBio Technology, Shanghai, China) for the isolation of total protein, and the BCA Protein Assay Kit (Innochem, Beijing, China) was utilized to measure the protein concentration. Thereafter, proteins (40 μg) were

**Table 1** Sequences of primers used for reverse transcription-quantitative PCR

| Genes | Sequence (5'→3') |
| --- | --- |
| CREB1 forward | AGCAGCTCATGCAACATCATC |
| CREB1 reverse | AGTCCTTACAGGAAGACTGAACT |
| RPL9 forward | AAGACCATTCTCAGCAATCAGAC |
| RPL9 reverse | TTACCCCACCATTTGTCAACC |
| GAPDH forward | AGGTCGGTGTGAACGGATTTG |
| GAPDH reverse | GGGGTCGTTGATGGCAACA |

separated by sodium dodecyl sulfate–polyacrylamide gel electrophoresis and blotted on a polyvinylidene difluoride membrane. After blocking with 5% skimmed milk for 2 h, the membrane was incubated overnight with primary antibodies against CREB1 (12208–1-AP, 1:3000; Proteintech, Rosemont, IL, USA), phosphorylated IκBα, IκBα (ab32518, 1:1000; Abcam, Shanghai, China), phosphorylated p65 (ab133462, 1:10000; Abcam), phosphorylated p65 (#3033, 1:1000; Cell Signaling, Shanghai, China), RPL9 (68054–1-Ig, 1:5000; Proteintech), GAPDH (10494–1-AP, 1:6000; Proteintech), Bax (ab32503, 1:1000; Abcam), Bcl-2 (ab196495, 1:1500; Abcam) and p65 (#8242, 1:1000; Cell Signaling Technology) at 4℃, and subsequently incubated with respective secondary antibodies for 2 h at room temperature. After washing with TBST (Sigma-Aldrich) three times, the bands were visualized by enhanced chemiluminescence reagent (Beyotime), and the intensity of blot was quantified by Image Lab 3.0 software (Bio-Rad, Hercules, CA, USA).

## Confocal Analysis

IVCs from control and model mice expressing GFP (green fluorescent protein) fluorescence were freshly excised and frozen sectioned. Airway sections were stained with DAPI (Beyotime) for nuclear staining. Confocal images were acquired using a confocal microscope (Olympus, Tokyo, Japan).

## Measurement of Inflammatory Cytokines

The collected venous plasma was centrifuged at 3000 r/min for 10 min at 4℃. The cells after indicated treatment were inoculated into a 96-well plate, and when reaching 70% confluence, the supernatant was collected. The levels of TNF-α, IL-1β, and IL-6 in serum and cells were assayed with commercially available ELISA kits (Cusabio Technology, Houston, TX, USA). The absorbance value at 450 nm was read via a microplate reader (Thermo Fisher Scientific).

## Cell Count Kit-8 (CCK-8) Assays

The transfected cells were inoculated into 96-well plates ($3 \times 10^3$ cells/well) and incubated overnight. The cell viability was assessed at 0, 24, 48 and 72 h via addition of detection buffer (100 μL medium containing 10 μL CCK-8 solution) at different time points. CCK-8 solution was obtained from (TopScience, Shanghai, China). After 2 h of incubation at 37℃, the absorbance at 450 nm was measured via a microplate reader (Thermo Fisher Scientific).

## Flow Cytometry

The cells were trypsinized using EDTA-free trypsin (Thermo Fisher-Scientific) and centrifuged. Thereafter, the cells were stained with Annexin-V-FITC (Sigma-Aldrich) for 30 min, and subsequently stained with propidium iodide (PI) (Sigma-Aldrich) for 15 min. Finally, flow cytometer (Thermo Fisher Scientific) was used to analyze cell apoptosis.

## Chromatin Immunoprecipitation (CHIP) Assays

This assay was conducted using a CHIP assay kit (Beyotime). The VECs were cross-linked with 1% formaldehyde and sonicated to shear DNA to lengths between 200–1000 base pairs. Thereafter, the cell lysates were incubated at 4℃ with protein A/G beads (MedChemExpress) coated with anti-CREB1 antibody (2 μg, Abcam) or IgG (2 μg, Abcam) overnight. Subsequently, the samples were washed and eluted followed by treatment with 5 M NaCl for heating and incubation with proteinase K (MedChemExpress) for 1 h. Finally, the bound DNA fragments were purified via a DNA Extraction Kit (Sigma-Aldrich) and analyzed by RT-qPCR.

## Luciferase Reported Assays

The promoter region of RPL9 was constructed into pGL3-Basic vector (HonorGene, Changsha, China) to obtain recombinant vector pGL3-RPL9-Wt. The mutation site of complementary sequence was designed based on pGL3-RPL9-Wt and was inserted into pMIR-reporter plasmid (Biovector Science, Beijing. China), and subsequently a recombinant vector RPL9-Mut was obtained. The promoter-Renilla luciferase reporter plasmid (Promega, Madison, WI, USA) of Renilla luciferase was used as an internal reference. The cells were incubated in 24-well plates ($3 \times 10^4$ cells/well). The overexpression plasmids of CREB1 were formed via cloning the corresponding full-length sequences into pcDNA3.1 vector (Youbio, Changsha. China), and empty vector was used as a negative control. Next, the recombinant plasmids were co-transfected with CREB1 overexpression vector or empty vector into the VECs. A dual luciferase reporter gene analysis system (Promega) was used to measure relative luciferase units after 48 h of transfection.

## Immunofluorescence Staining

The VECs were seeded in 24-well plates with poly-L-lysine-coated coverslips ($2 \times 10^5$ cells/ml). After indicated interventions, the coverslips received 2-time PBS washings, 15-min 4% paraformaldehyde treatment, and 0.1% Triton X-100 permeabilization (Sigma-Aldrich). The slides were washed and subsequently incubated overnight with a primary antibody against p65 (sc-8008, 1:1000;

Santa Cruz, Beijing, China) followed by incubation with the corresponding secondary antibody for 1 h at room temperature. Thereafter, the nuclear was stained by DAPI for 5 min. Finally, the slides were sealed with an anti-fluorescence quenching sealant (Beyotime) and observed via a confocal laser scanning microscope (Olympus).

## Statistics Analysis

All experiments were performed at least three independent repeats. Statistical analysis was analyzed using Graph-Pad Prism 8 (GraphPad Software, San Diego, CA, USA). Data were described as the mean ± standard deviation. One-way analysis of variance (ANOVA) followed by Tukey's post hoc analysis and Student's t test were used for comparison analyses. $p < 0.05$ was considered statistically significant.

## Results

### CREB1 Expression is Decreased in Thrombotic IVC of DVT Rats

An experimental DVT model was established via IVC stenosis, and the IVC containing thrombus was harvested and weighed at 24 h post-surgery. We found that IVC stenosis significantly increased the length and weight of thrombus (Fig. 1A-B). Then, the IVC sections were stained with hematoxylin and eosin to examine the pathological changes of venous thrombosis, and we found that the IVC wall structure was intact without thrombosis in the vascular lumen of sham-operated rats, whereas IVC stenosis led to a full thrombosis in DVT rats (Fig. 1C). Next, the levels of proinflammatory cytokines (TNF-α, IL-1β, and IL-6) in serum samples collected from sham-operated rats and DVT rats were measured by ELISA kits.



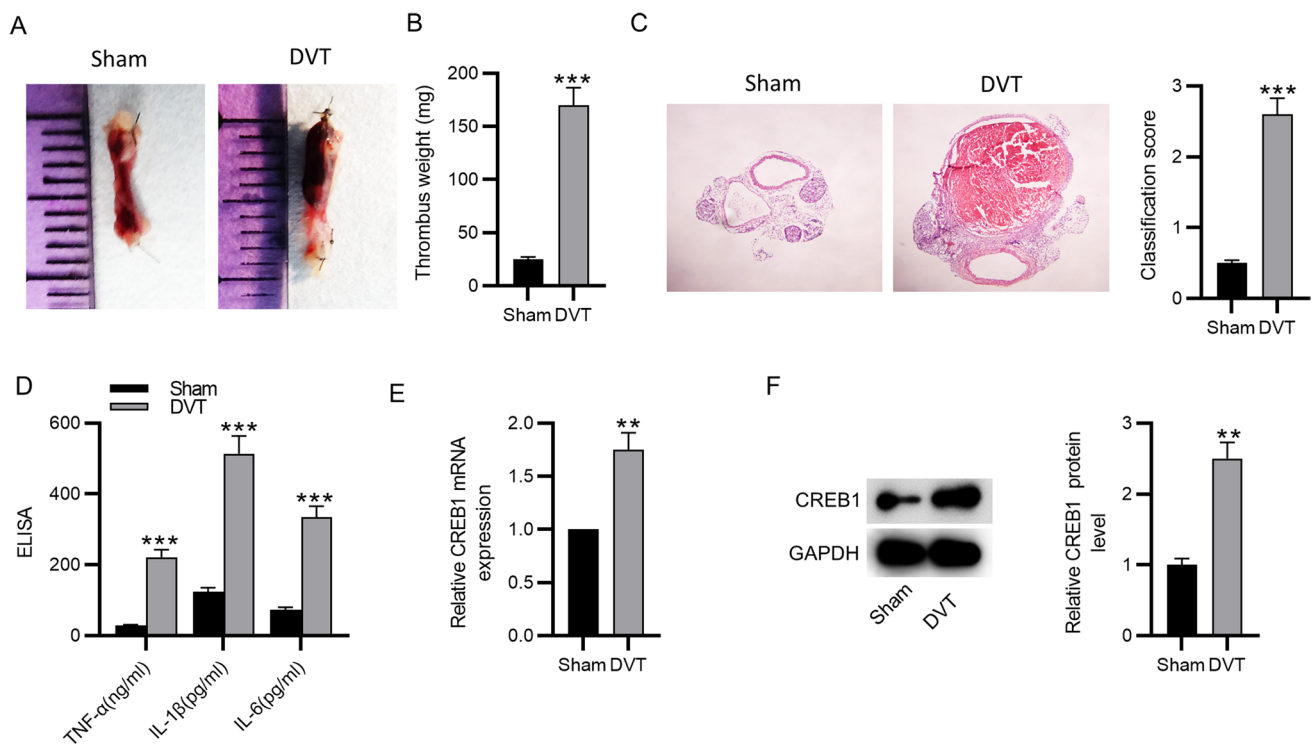**Fig. 1** CREB1 expression is upregulated in venous wall tissues of DVT rats. (**A**) DVT was induced by IVC stenosis in SD rats, and the sham operation included the same surgical procedure without IVC stenosis. The IVCs were collected at 24 h post-surgery. Representative images of IVCs isolated from sham-operated and model rats were photographed ($n = 5$). (**B**) The weights of IVC thrombosis ($n = 5$, ***$p < 0.001$ with Student's t test). (**C**) The thrombosis in the rats after DVT model establishment was observed by hematoxylin and eosin staining. The thrombosis was assessed and recorded by pathological professionals according to the histological examination of thrombus grading evaluation criteria. 0 represents no thrombus, 1 represents vascular obstruction < 50%, 2 represents vascular obstruction > 50% and 3 represents complete vascular obstruction ($n = 5$, ***$p < 0.001$ with Student's t test). (**D**) The levels of TNF-α, IL-1β, and IL-6 in serum were measured by ELISA ($n = 5$, ***$p < 0.001$ with Student's t test). (**E**) The mRNA level of CREB1 in the thrombotic IVC of DVT rats was measured by RT-qPCR ($n = 4$, **$p < 0.01$ with Student's t test). (**F**) The protein level of CREB1 was evaluated by western blotting ($n = 4$, **$p < 0.01$ with Student's t test). Data were expressed as mean ± standard deviation

The experimental data revealed that IVC stenosis resulted in significant increases in the levels of these proinflammatory cytokines (Fig. 1D). Thereafter, the mRNA and protein levels of CREB1 in the IVCs were measured by RT-qPCR and western blotting. The results showed that the DVT rats presented with significantly higher expression of CREB1 compared to the sham-operated rats (Fig. 1E-F). Above findings show that IVC stenosis can induce thrombosis in rats, and CREB1 is highly expressed in the IVCs of DVT rats.

## CREB1 Depletion Suppresses Thrombosis and Inflammation in DVT Rats

Considering the upregulation of CREB1 in DVT rats, we effectively knocked it down by injecting 20 ml transfection compound containing 400 pmol of si-CREB1 through the tail vein into the DVT rats. To test whether si-CREB1 was able to exert functions in the DVT rats, confocal microscopy was used to confirm the proper insertion of si-CREB1 (Fig. 2A). The knockdown efficiency of si-CREB1 on
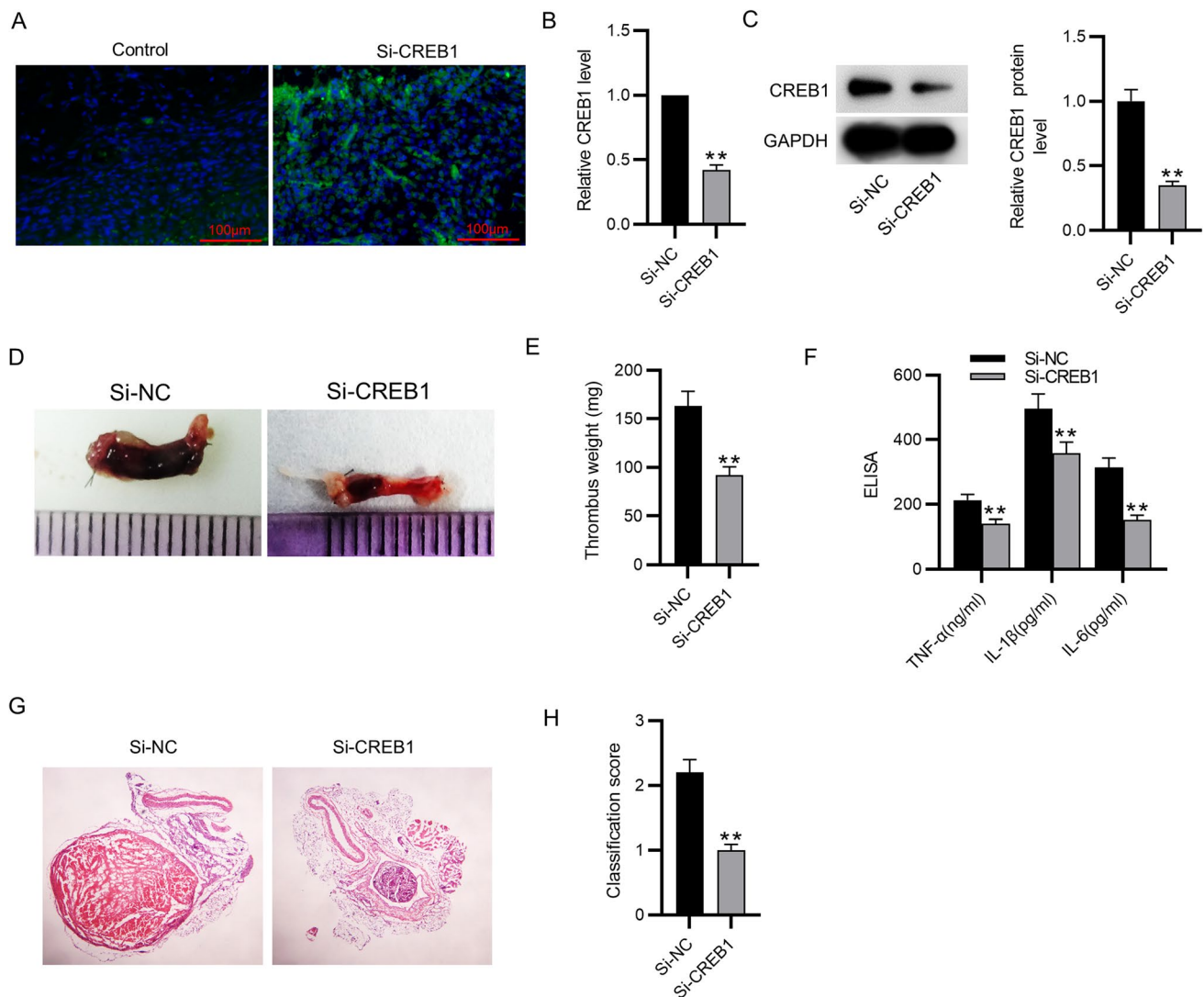


**Fig. 2** CREB1 depletion suppresses thrombosis and inflammation in DVT rats. (**A**) The CREB1 siRNA-GFP signal in freshly harvested IVCs ($n = 3$). (**B-C**) The delivery efficiency of si-CREB1 was detected by RT-qPCR and western blotting ($n = 4$, $**p < 0.01$ with Student's $t$ test). (**D**) Representative images of thrombotic IVC isolated from DVT rats in the si-CREB1 and the si-NC groups ($n = 5$). (E) Thrombus weight ($n = 5$, $**p < 0.01$ with Student's $t$ test). (**F**) The levels of TNF-α, IL-1β, and IL-6 in serum were assessed by ELISA ($n = 5$, $**p < 0.01$ with Student's $t$ test). (**G**) Representative images of hematoxylin and eosin stained IVCs ($n = 5$). (**H**) Classification score ($n = 5$, $**p < 0.01$ with Student's $t$ test). Data were expressed as mean ± standard deviation

CREB1 expression in IVCs of DVT rats were confirmed by RT-qPCR and western blotting (Fig. 2B-C). Then, the IVCs containing thrombus were collected from DVT rats injected with si-CREB1 or si-NC. The length and weight of thrombus in the vascular lumen were significantly declined with CREB1 knockdown (Fig. 2D-E). Afterwards, the levels of TNF-α, IL-1β, and IL-6 were analyzed by ELISA. Compared with the si-NC group, the contents of these pro-inflammatory cytokines were remarkably reduced in the si-CREB1 group (Fig. 2F). Finally, the results of hematoxylin and eosin staining revealed that CREB1 knockdown alleviated the IVC stenosis-induced thrombosis and decreased the thrombosis grading score (Fig. 2G-H). These results indicate that CREB1 knockdown mitigates thrombosis and inflammation in DVT rats.

## CREB1 Knockdown Inhibits Inflammatory Response and Apoptosis of Rat VECs

To further explore the in vitro effects of CREB1 on inflammation, VECs were isolated and transduced with si-CREB1. The knockdown efficiency was confirmed by RT-qPCR and western blotting (Fig. 3A-B). Then, we assessed the in vitro roles of CREB1 knockdown in viability, apoptosis and
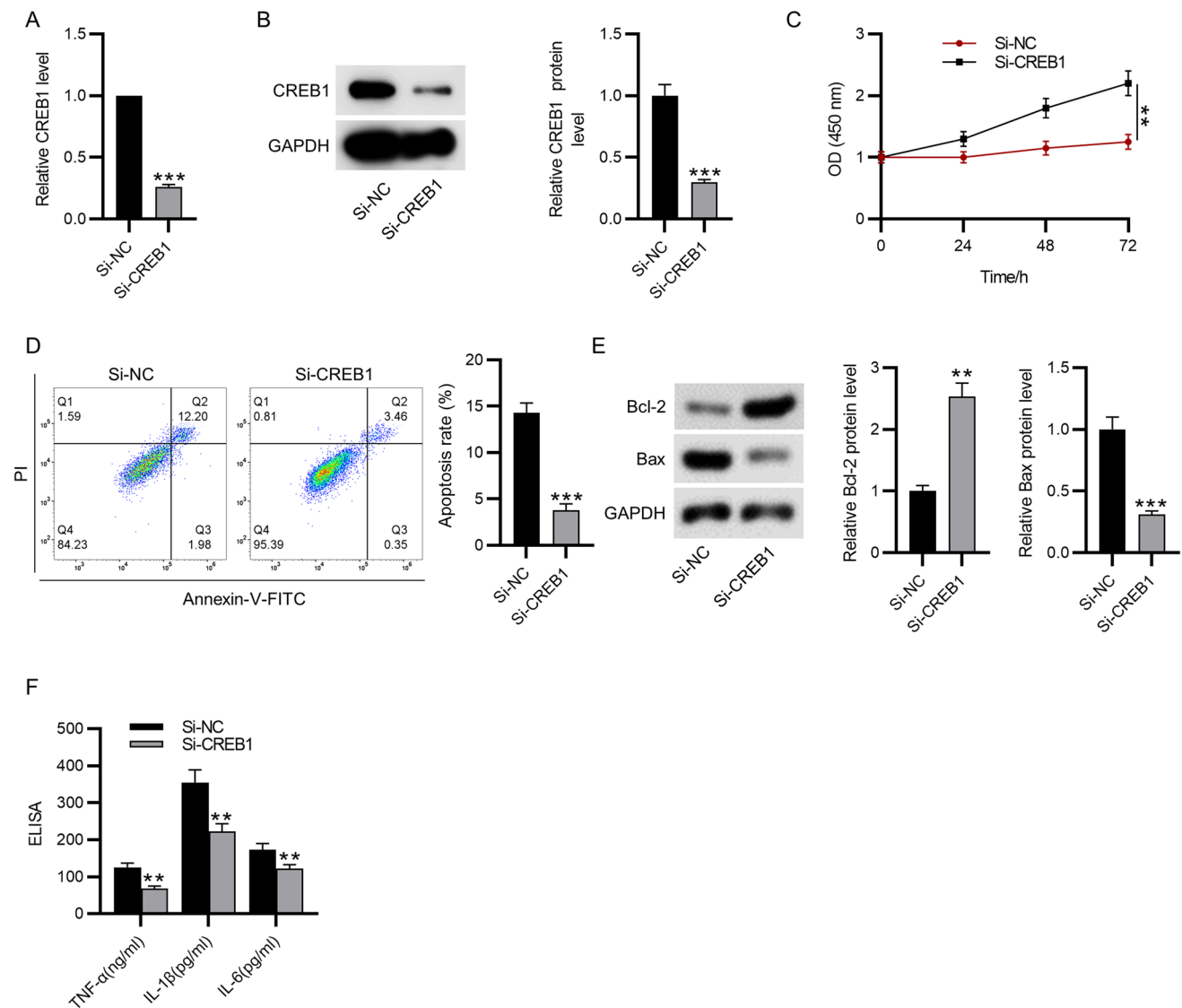


**Fig. 3** The apoptosis and inflammatory responses are inhibited in CREB1-silenced vascular endothelial cells. (**A-B**) The mRNA and protein levels of CREB1 in VECs transfected with si-NC or si-CREB1 were measured by RT-qPCR and western blotting ($n=3$, ***$p<0.001$ with Student's $t$ test). (**C**) The viability of VECs was assessed by CCK-8 assays ($n=5$, **$p<0.01$ with Student's $t$ test). (**D**) The apoptosis of VECs was estimated by flow cytometry ($n=5$, ***$p<0.001$ with Student's $t$ test). (**E**) The protein levels of Bcl-2 and Bax were measured by western blotting ($n=3$, ***$p<0.001$ with Student's $t$ test). (**F**) The levels of TNF-α, IL-1β, and IL-6 in VECs were measured by ELISA ($n=3$, **$p<0.01$ with Student's $t$ test). Data were expressed as mean ± standard deviation

inflammation of VECs. As CCK-8 revealed, the viability of si-CREB1-transfected VECs was significantly increased than that of si-NC-transfected VECs (Fig. 3C). The apoptosis rate of VECs transfected with si-CREB1 was markedly reduced compared to that of VECs transfected with si-NC, as shown by flow cytometry (Fig. 3D). Consistently, CREB1 knockdown increased Bcl-2 (anti-apoptotic gene) protein level and decreased Bax (pro-apoptotic gene) protein level in VECs (Fig. 3E). Finally, ELISA demonstrated that the si-CREB1-treated VECs expressed lower levels of TNF-α, IL-1β, and IL-6 than those treated with si-NC (Fig. 3F). These results show that CREB1 knockdown can suppress apoptosis and inflammation in VECs.

## CREB1 Activates RPL9 at the Transcription Level in Rat VECs

The mRNA and protein levels of RPL9 were decreased in VECs in the context of CREB1 knockdown (Fig. 4A-B). Then, we measured RPL9 expression in the IVCs of sham-operated and DVT rats. The results showed that the DVT rats expressed higher RPL9 level than the sham-operated rats (Fig. 4C-D). UCSC (https://genome.ucsc.edu/) and JASPAR (https://jaspar.genereg.net) indicated the potential CREB1 binding sites on RPL9 promoter (Fig. 4E). Chromatin fragments were immunoprecipitated using anti-CREB1 antibody with anti-IgG antibody as negative control, and the precipitated DNA fragments were amplified by RT-qPCR. The results showed the successful recruitment of CREB1 by binding site 1 of RPL9 promoter but not binding site 2 and 3 (Fig. 4F). Finally, to confirm the functional link between the CREB1-binding site and RPL9 promoter activity, wild type (pGL3-RPL9 promoter-Wt) and mutant type (pGL3-RPL9 promoter-Mut) were designed and synthesized. The results of luciferase reporter assays showed that significantly increased luciferase activity upon RPL9 binding could be observed in cells transfected with CREB1 overexpression vector. When the binding sites were mutated, CREB1 overexpression was unable to induce any activity within the RPL9 promoter. (Fig. 4G). These results suggest that CREB1 transcriptionally activates RPL9 dependent of the 602–609(-) in RPL9 promoter area and positively regulates its expression.

## RPL9 Upregulation Abolishes the Inhibitory Effects of CREB1 Knockdown on Apoptosis and Inflammation of Rat VECs

We effectively overexpressed RPL9 in VECs, and RT-qPCR and western blotting were performed to measure the mRNA and protein levels of RPL9 in RPL9 overexpressed VECs (Fig. 5A-B). Then, we assessed the effect of RPL9 overexpression on cell viability, apoptosis and inflammation. As

CCK-8 assays and flow cytometry revealed, RPL9 overexpression abolished the viability enhancing effect and apoptosis suppressive effect of CREB1 knockdown on VECs (Fig. 5C-D). Concomitantly, RPL9 overexpression significantly reduced Bcl-2 protein level and increased Bax protein level in VECs with CREB1 knockdown (Fig. 5E). Finally, in the context of CREB1 knockdown, RPL9 overexpression increased the levels of TNF-α, IL-1β, and IL-6 (Fig. 5F). Taken together, RPL9 elevation reverses the si-CREB1-induced inhibition in apoptosis and inflammation.

## CREB1 Knockdown Transcriptionally Regulates RPL9 to Inactivate the NF-κB Pathway in Rat VECs

As western blotting indicated, CREB1 knockdown decreased the phosphorylation level of IκBα and p65, which was recovered by RPL9 upregulation. Notably, QNZ effectively inhibited the activation of NF-κB pathway (Fig. 6A). Then, immunofluorescence staining was conducted to detect p65 location. The results showed that CREB1 knockdown reduced the nuclear translocation of p65, whereas RPL9 overexpression abolished the si-CREB1-induced inhibition in p65 nuclear translocation. Simultaneously, QNZ effectively declined the nuclear translocation of p65 (Fig. 6B). Next, we examined the effect of QNZ on cell viability, apoptosis and inflammation in VECs co-transfected with si-CREB1 and RPL9 overexpression vector. As shown by CCK-8 assays and flow cytometry, the QNZ-challenged VECs presented higher viability and lower apoptotic rate than that of VECs transfected with si-CREB1 or combination of si-CREB1 and RPL9 overexpression vector (Fig. 6C-D). The results of western blotting confirmed the apoptosis inhibitory effect of QNZ, as evidenced by increased Bcl-2 protein level and decreased Bax protein level (Fig. 6E). Moreover, QNZ treatment also inhibited the production of proinflammatory cytokines in VECs (Fig. 6F). The scientific schematic diagram depicting the mechanisms by which CREB1 promotes inflammation during the process of DVT was presented in Fig. 7. In conclusion, CREB1 silencing alleviates thrombosis and inflammation in IVC stenosis-induced DVT rats by transcriptionally regulating RPL9 and inactivating the NF-κB signaling.

## Discussion

Thrombosis induces the release of inflammatory cytokines, which accelerate hypercoagulability state and cause endothelial damage, exacerbating DVT [31]. In the current study, experimental DVT was induced by IVC stenosis, and we found that IVC stenosis stimulated thrombosis formation, increased infiltration of inflammatory cytokines, and increased CREB1 level. Downregulation of CREB1 inhibits
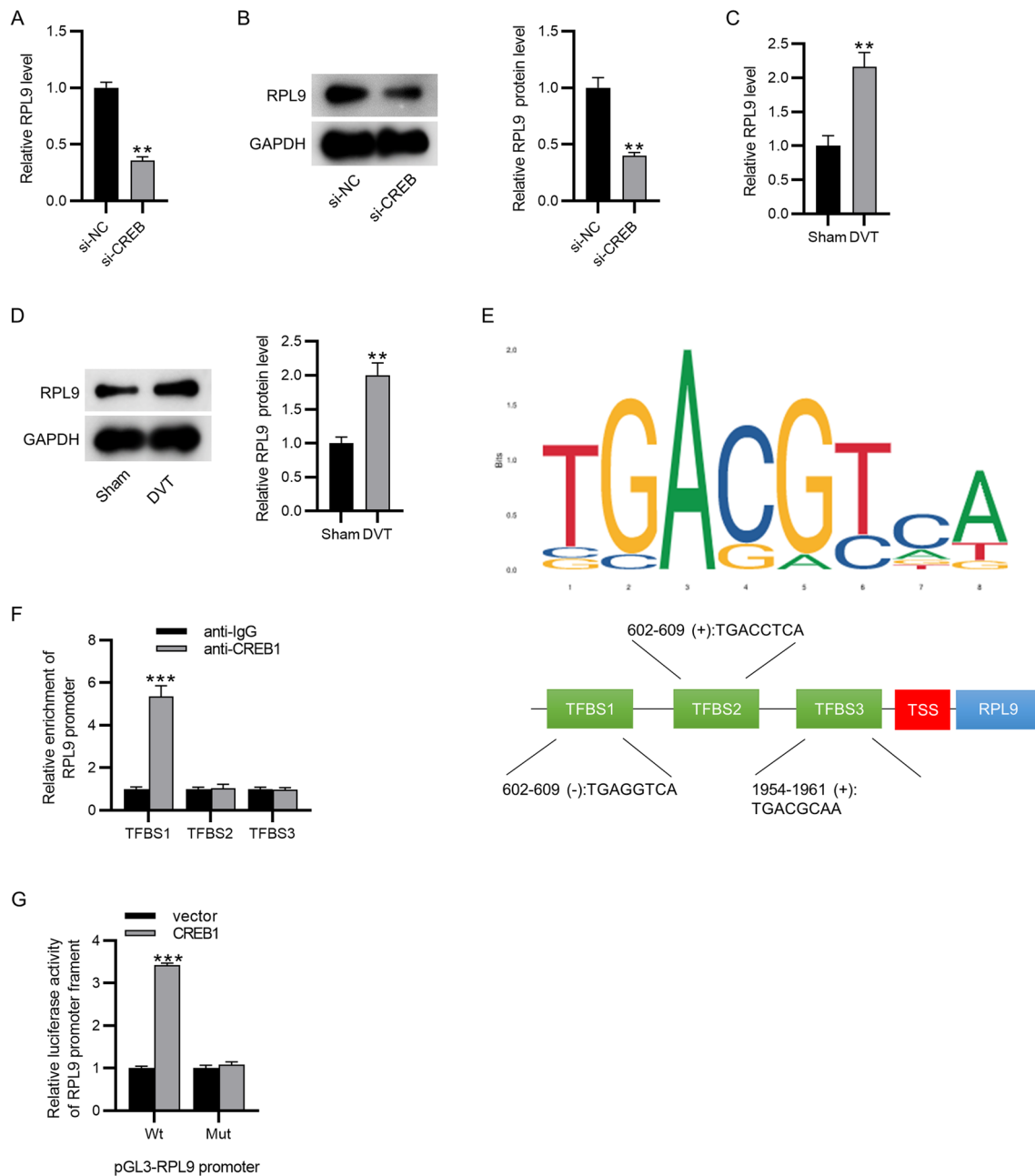
**Fig. 4** CREB1 activates RPL9 at the transcription level. (**A-B**) RT-qPCR and western blotting were conducted to assess the mRNA and protein levels of RPL9 in the context of CREB1 knockdown ($n=3$, **$p<0.01$ with Student's $t$ test). (**C-D**) The mRNA and protein levels of RPL9 in sham-operated and DVT rats ($n=3$, **$p<0.01$ with Student's $t$ test). (**E**) A schematic map to show the potential binding of CREB1 on RPL9 promoter region. (**F**) The binding affinity of CREB1 and RPL9 was analyzed by ChIP assays ($n=5$, ***$p<0.001$ with Student's $t$ test). (**G**) Luciferase reporter assays were used to explore the validity of putative CREB1 binding sites for RPL9 ($n=5$, ***$p<0.001$ with Student's $t$ test). Data were expressed as mean ± standard deviation

cell proliferation and aggravates inflammation in osteoarthritis [32], blocks the protective effects of CaMKIV on inflammatory response and mitochondrial dysfunction [33]. CREB1 elevation suppresses the progression of ulcerative colitis via through attenuation of inflammation in dextran sodium sulfate-treated mice [34], curtails the release of proinflammatory proteins in postoperative neurocognitive disorders [35]. The present study showed that CREB1 silencing decreased the release of pro-inflammatory cytokines in blood samples and VECs collected from model rats. VECs are associated with DVT development, and cellular apoptosis of VECs inhibits the release of active substances and
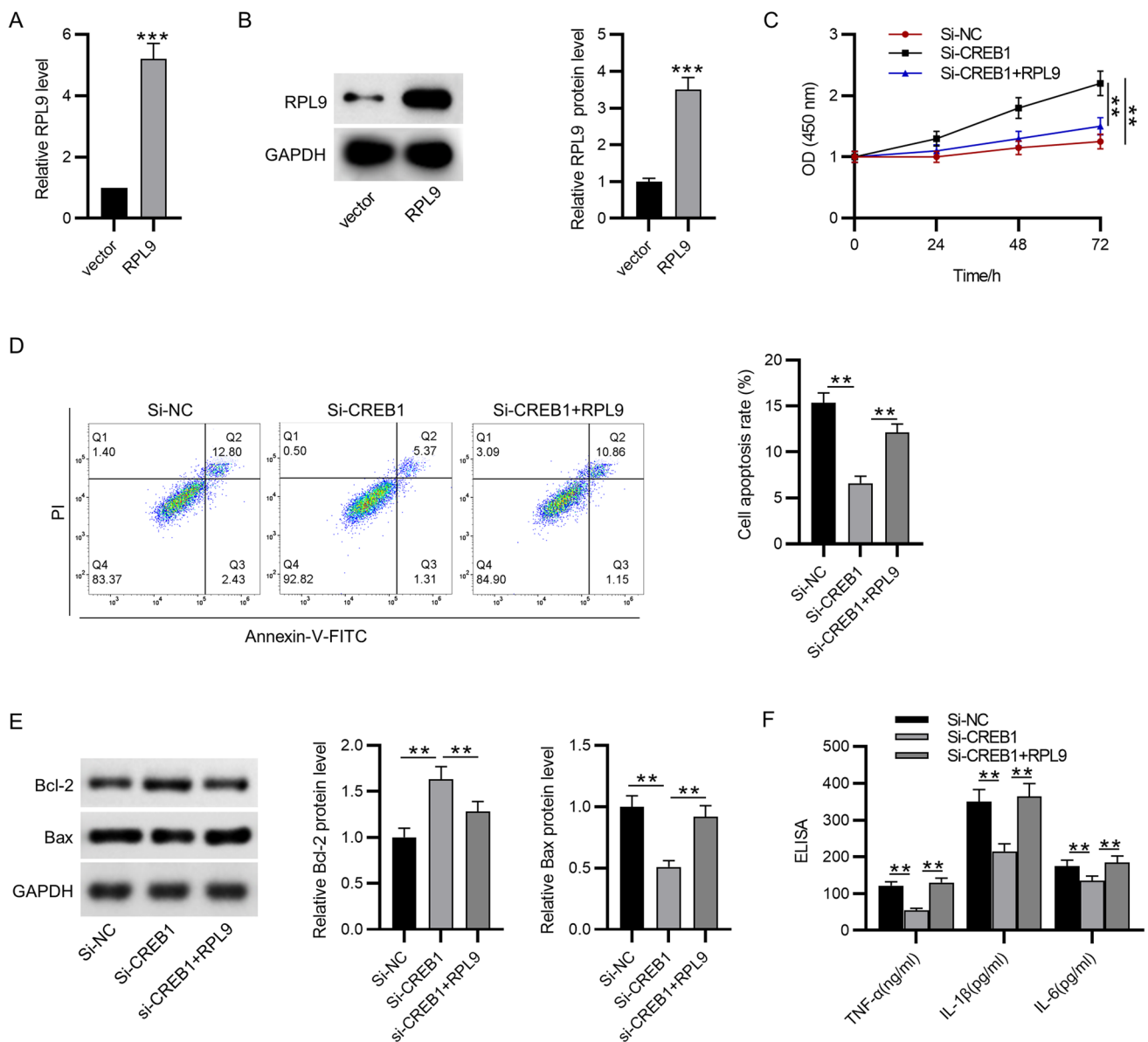
**Fig. 5** RPL9 upregulation abolishes the inhibitory effects of CREB1 knockdown on apoptosis and inflammation of VECs. (**A-B**) RPL9 was overexpressed by pcDNA3.1 vector, and the overexpression efficiency was determined by RT-qPCR and western blotting ($n = 3$, ***$p < 0.001$ with Student's $t$ test). (**C**) The viability of VECs transfected with si-NC, si-CREB1, and si-CREB1 + RPL9 was assessed by CCK-8 assays ($n = 5$, **$p < 0.01$ with one-way ANOVA followed by Tukey's post hoc test). (**D**) The apoptosis of VECs was determined by flow cytometry ($n = 5$, **$p < 0.01$ with one-way ANOVA followed by Tukey's post hoc test). (E) The protein levels of Bcl-2 and Bax were measured by western blotting ($n = 3$, **$p < 0.01$ with one-way ANOVA followed by Tukey's post hoc test). (F) The levels of TNF-α, IL-1β, and IL-6 in VECs were evaluated by ELISA ($n = 3$, **$p < 0.01$ with one-way ANOVA followed by Tukey's post hoc test). Data were expressed as mean ± standard deviation

impairs defense functions in blood vessels, eventually facilitating DVT [36]. Induction of human endothelial stromal cell apoptosis is an effective therapeutic approach for endometriosis [37, 38], and Feng Y report that CREB1 silencing enhances endometrial stromal cell apoptosis [39]. CREB1 upregulation reduces the infarct-induced cardiomyocytes apoptosis and attenuates cardiac dysfunction after acute myocardial infarction [40]. CREB1 can restore the heart

failure-induced cardiomyocyte apoptosis and alleviate cardiac dysfunction in rats with heart failure [41]. However, this study showed that CREB1 knockdown increased the viability and reduced the apoptosis of VECs isolated from rats with DVT, and the results of this study was similar to a previous report of Hu Z et al. that CREB1 silencing reduces the apoptosis of lung epithelial cells [26]. We postulated that the differences among studies are attributed to different cell
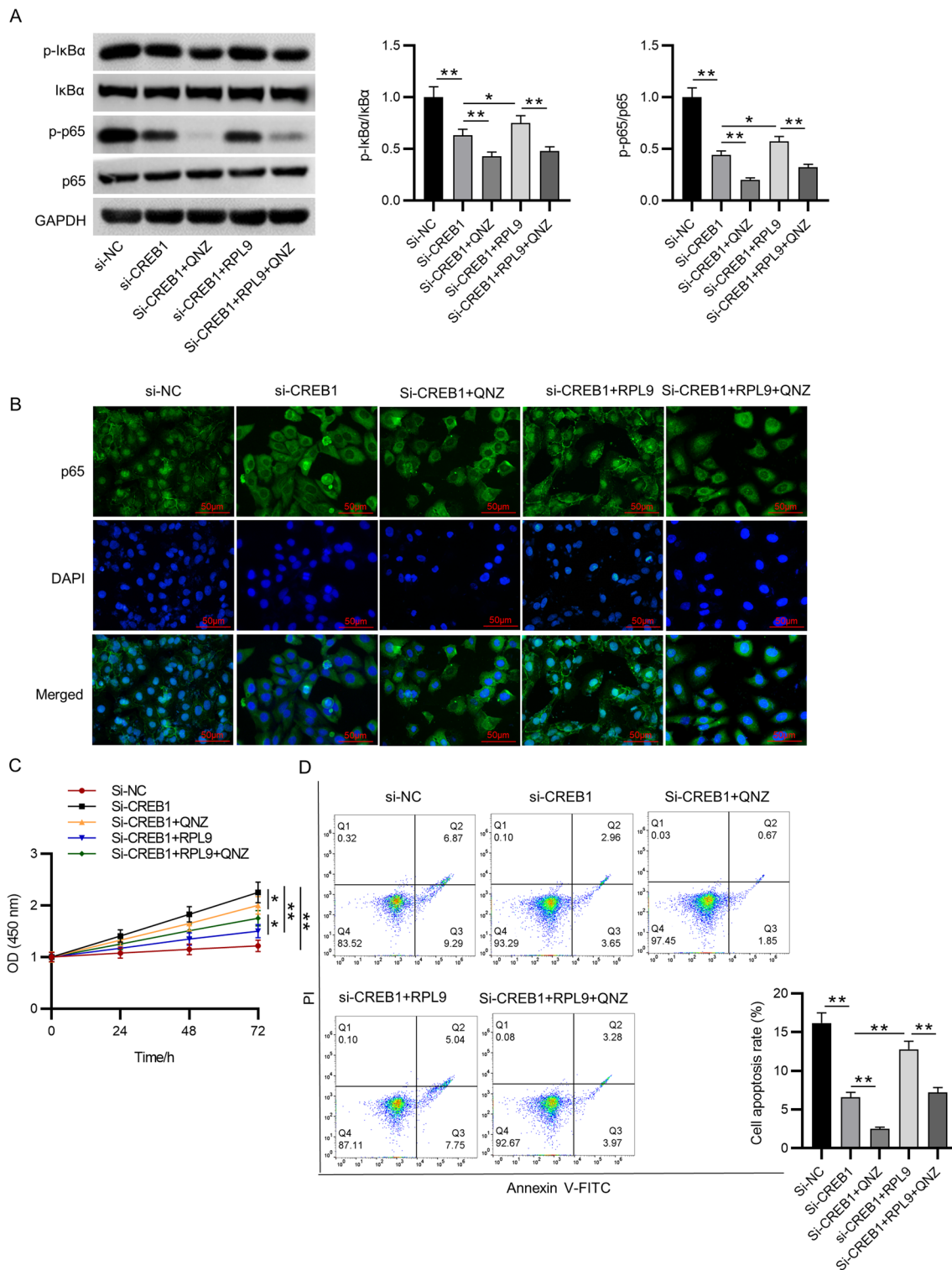
**Fig. 6** CREB1 silencing inactivates the NF-κB signaling. (**A**) Western blotting was performed to measure the protein levels of phosphorylated IκBα and phosphorylated p65 ($n=3$, \*\*$p<0.01$, \*\*\*$p<0.001$ with one-way ANOVA followed by Tukey's post hoc test). (**B**) the p65 location was determined by Immunofluorescence staining (scale bar$=50$ μm). (**C**) The viability of VECs was detected by CCK-8 assays ($n=5$, \*\*$p<0.01$ with one-way ANOVA followed by Tukey's post hoc test). (**D**) The apoptosis of VECs was estimated by flow cytometry ($n=5$, \*\*$p<0.01$ with one-way ANOVA followed by Tukey's post hoc test). (**E**) The protein levels of Bcl-2 and Bax were measured by western blotting ($n=3$, \*\*$p<0.01$ with one-way ANOVA followed by Tukey's post hoc test). (**F**) The levels of TNF-α, IL-1β, and IL-6 in VECs were evaluated by ELISA ($n=3$, \*\*$p<0.01$ with one-way ANOVA followed by Tukey's post hoc test). Data were expressed as mean$\pm$standard deviation
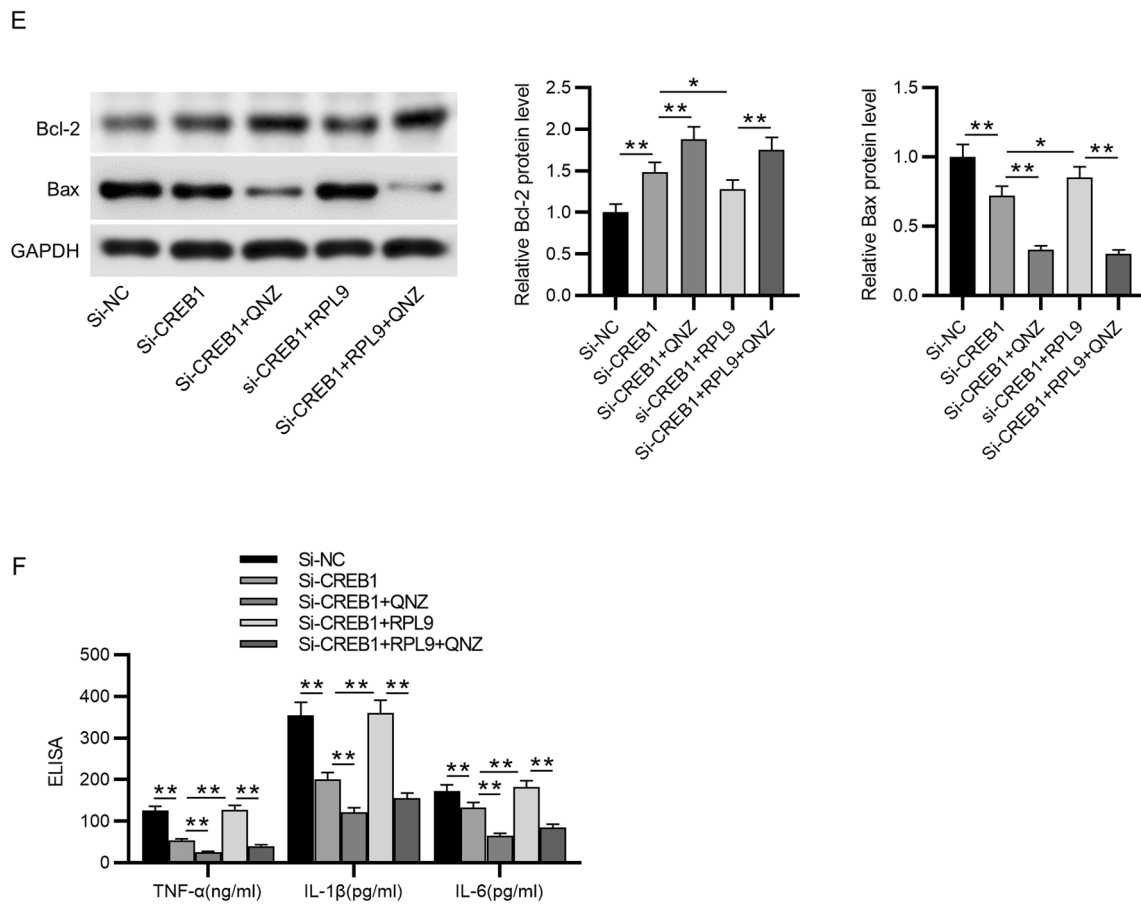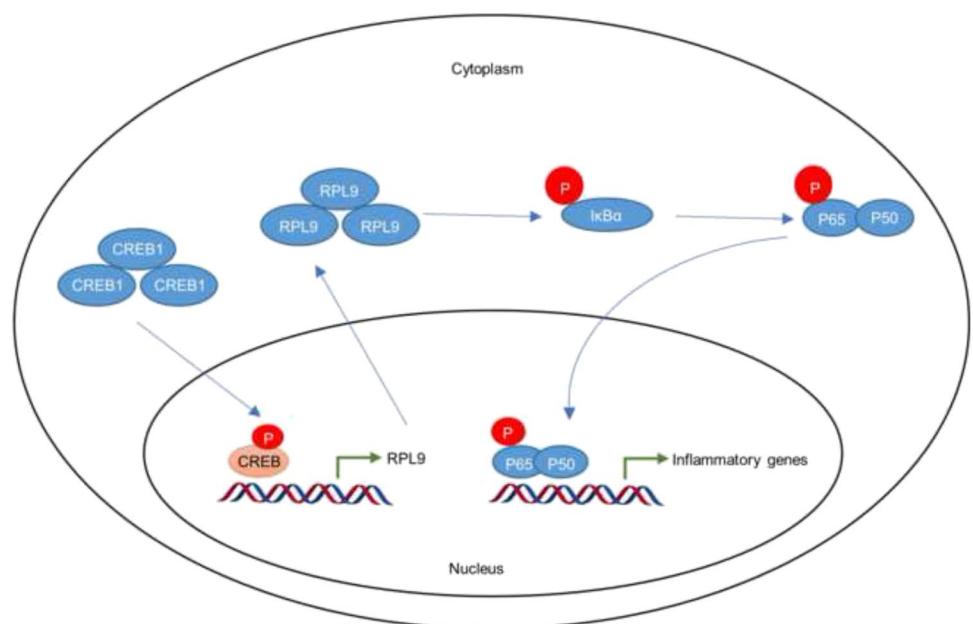
E



F



**Fig. 6** (continued)

**Fig. 7** The scientific schematic diagram depicts the mechanisms by which CREB1 affects inflammation during the process of DVT

types, specific pathological processes, and distinct underlying mechanisms.

CREB1 and RPL9 are upregulated in blood samples of patients with VTE compared to healthy volunteers [23, 24]. By estimating the prevalence in Saudi Arabia, blood RPL9 can be tracked in patients with thromboembolism [42], and RPL9 level is upregulated in both recurrent VTE and single VTE [43]. Watanabe M et al. articulate that RPL9 is identified as a novel type of damage-associated molecular pattern molecule with a regulatory role in the proinflammatory response [44]. Knockdown of RPL9 inhibits the innate immune response and increases proliferation of Salmonella in neutrophils, which allows the bacteria to successfully proliferate intracellularly [45]. As reported, CREB1 can regulate the expression of RPL9 in VTE [24]. In the current study, we found that RPL9 level was lower in experimental DVT model compared to that in sham-operated rats, and CREB1 knockdown downregulated RPL9 level in VECs. The binding sites and sequences between CREB1 and RPL9 promoter was predicted by bioinformatics analysis, and CHIP and luciferase reporter assays were performed to verify the regulatory relationship. Collectively, CREB1 promotes RPL9 transcription and positively regulated its expression. Moreover, RPL9 upregulation reversed the inhibitory effects of CREB1 knockdown on cell apoptosis and inflammation.

NF-κB is a common transcription factor associated with inflammation, leading to stimulation of inflammatory response and cell apoptosis [46]. Inhibition of NF-κB signaling is beneficial to improve DVT as evidenced by previous studies. For example, rivaroxaban inactivates the NF-κB signaling to attenuate thrombosis in rats with DVT [47]. Additionally, paeoniae radix rubra prevents DVT by ameliorating inflammation by inhibiting NF-κB signaling [48]. CREB1, a common transcription factor, can transcriptionally activate lymphotoxin beta receptor (LTBO) and histone deacetylase 2 (HDAC2) to promote the activation of NF-κB pathway [25, 26]. A previous study suggests that RPL9 depletion can result in inactivation of NF-κB signaling in colorectal carcinoma [27]. The current study demonstrated that CREB1 knockdown attenuated phosphorylation of IκBα and p65 and inhibited nuclear translocation of p65, whereas RPL9 overexpression had the opposite effect. Moreover, inhibition of NF-κB pathway reduced cell apoptosis and inflammation.

In conclusion, this study illustrated that CREB1 was highly expressed in experimental DVT model and CREB1 knockdown attenuated cell apoptosis and inflammation and reduced thrombosis by downregulating RPL9 expression at the transcriptional level and blocking the NF-κB signaling in VECs. There are limitations to this study. First, the anti-inflammatory and anti-apoptotic effects of CREB1 have been described in previous studies; thus, more studies are required to confirm its roles in DVT. Second, further investigation in more underlying mechanisms by which CREB1 affects DVT progression are required. Despite these limitations, our findings suggest that CREB1 may play an important role in the development of DVT and that targeting of CREB1 may be an attractive option for exploiting a net-line molecular therapy of DVT.

**Data Availability** The data that support the findings of this study are available on request from the corresponding author upon reasonable request.

## Declarations

**Ethical Statement** All experiments involving animals were approved by the Animal Ethics Committee of The Central Hospital of Wuhan, Tongji Medical College, Huazhong University of Science and Technology, and all experimental protocols strictly followed the Guide for the Care and Use of Laboratory Animals published by the National Institutes of Health (NIH publication no.85–23, revised 1996).

**Competing Interests** The authors declare that they have no competing interests.

## References

1. Wang TY, Sakamoto JT, Nayar G, Suresh V, Loriaux DB, Desai R, et al. Independent Predictors of 30-Day Perioperative Deep Vein Thrombosis in 1346 Consecutive Patients After Spine Surgery. World Neurosurg. 2015;84(6):1605–12.

2. Sforza M, Husein R, Saghir R, Saghir N, Okhiria R, Okhiria T, et al. Deep Vein Thrombosis (DVT) and Abdominoplasty: A Holistic 8-Point Protocol-Based Approach to Prevent DVT. Aesthet Surg J. 2021;41(10):Np1310-np20.

3. Sevuk U, Altindag R, Bahadir MV, Ay N, Demirtas E, Ayaz F. Value of platelet indices in identifying complete resolution of thrombus in deep venous thrombosis patients. Indian J Hematol Blood Trans : an official journal of Indian Society of Hematology and Blood Transfusion. 2015;31(1):71–6.

4. Santin BJ, Lohr JM, Panke TW, Neville PM, Felinski MM, Kuhn BA, et al. Venous duplex and pathologic differences in thrombus characteristics between de novo deep vein thrombi and endovenous heat-induced thrombi. J Vasc Surg Venous Lymphat Disord. 2015;3(2):184–9.

5. Cheng Z, Jia W, Tian X, Jiang P, Zhang Y, Li J, et al. Cotinine inhibits TLR4/NF-κB signaling pathway and improves deep vein thrombosis in rats. Biosci Rep 2020;40(6)

6. Harter K, Levine M, Henderson SO. Anticoagulation drug therapy: a review. West J Emerg Med. 2015;16(1):11–7.

7. Bagot CN, Arya R. Virchow and his triad: a question of attribution. Br J Haematol. 2008;143(2):180–90.

8. Stark K, Philippi V, Stockhausen S, Busse J, Antonelli A, Miller M, et al. Disulfide HMGB1 derived from platelets coordinates venous thrombosis in mice. Blood. 2016;128(20):2435–49.

9. Luther N, Shahneh F, Brähler M, Krebs F, Jäckel S, Subramaniam S, et al. Innate Effector-Memory T-Cell Activation Regulates Post-Thrombotic Vein Wall Inflammation and Thrombus Resolution. Circ Res. 2016;119(12):1286–95.

10. Swystun LL, Liaw PC. The role of leukocytes in thrombosis. Blood. 2016;128(6):753–62.

11. Martinod K, Wagner DD. Thrombosis: tangled up in NETs. Blood. 2014;123(18):2768–76.

12. Budnik I, Brill A. Immune Factors in Deep Vein Thrombosis Initiation. Trends Immunol. 2018;39(8):610–23.

13. Malaponte G, Signorelli SS, Bevelacqua V, Polesel J, Taborelli M, Guarneri C, et al. Increased Levels of NF-kB-Dependent Markers in Cancer-Associated Deep Venous Thrombosis. PLoS One. 2015;10(7):e0132496.

14 Du T, Tan Z. Relationship between deep venous thrombosis and inflammatory cytokines in postoperative patients with malignant abdominal tumors. Brazilian J Med Biol Res Revista brasileira de pesquisas medicas e biologicas. 2014;47(11):1003–7.

15. Liu H, Li P, Lin J, Chen W, Guo H, Lin J, et al. Danhong Huayu Koufuye prevents venous thrombosis through antiinflammation via Sirtuin 1/NF-κB signaling pathway. J Ethnopharmacol. 2019;241:111975.

16. Zhou H, Li N, Yuan Y, Jin YG, Guo H, Deng W, et al. Activating transcription factor 3 in cardiovascular diseases: a potential therapeutic target. Basic Res Cardiol. 2018;113(5):37.

17. Zhang Z, Yin D, Wang Z. Contribution of hypoxia-inducible factor-1α to transcriptional regulation of vascular endothelial growth factor in bovine developing luteal cells. Animal Sci J Nihon chikusan Gakkaiho. 2011;82(2):244–50.

18. Evans CE, Humphries J, Waltham M, Saha P, Mattock K, Patel A, et al. Upregulation of hypoxia-inducible factor 1 alpha in local vein wall is associated with enhanced venous thrombus resolution. Thromb Res. 2011;128(4):346–51.

19. Wang Y, Xu J, Chen J, Fan X, Zhang Y, Yu W, et al. Promoter variants of VTN are associated with vascular disease. Int J Cardiol. 2013;168(1):163–8.

20. Wang B, Wang M, Jia S, Li T, Yang M, Ge F. Systematic Survey of the Regulatory Networks of the Long Noncoding RNA BANCR in Cervical Cancer Cells. J Proteome Res. 2022;21(4):1137–52.

21. Kuijpers MJ, de Witt S, Nergiz-Unal R, van Kruchten R, Korporaal SJ, Verhamme P, et al. Supporting roles of platelet thrombospondin-1 and CD36 in thrombus formation on collagen. Arterioscler Thromb Vasc Biol. 2014;34(6):1187–92.

22. Prakash P, Kulkarni PP, Chauhan AK. Thrombospondin 1 requires von Willebrand factor to modulate arterial thrombosis in mice. Blood. 2015;125(2):399–406.

23. Su Y, Li Q, Zheng Z, Wei X, Hou P. Identification of genes, pathways and transcription factor-miRNA-target gene networks and experimental verification in venous thromboembolism. Sci Rep. 2021;11(1):16352.

24. Gao LN, Li Q, Xie JQ, Yang WX, You CG. Immunological analysis and differential genes screening of venous thromboembolism. Hereditas. 2021;158(1):2.

25. Pan L, Niu Z, Gao Y, Wang L, Liu Z, Liu J, et al. Silencing of CREB Inhibits HDAC2/TLR4/NF-κB Cascade to Relieve Severe Acute Pancreatitis-Induced Myocardial Injury. Inflammation. 2021;44(4):1565–80.

26. Hu Z, Zhou G. CREB1 Transcriptionally Activates LTBR to Promote the NF-κB Pathway and Apoptosis in Lung Epithelial Cells. Comput Math Methods Med. 2022;2022:9588740.

27. Baik IH, Jo GH, Seo D, Ko MJ, Cho CH, Lee MG, et al. Knockdown of RPL9 expression inhibits colorectal carcinoma growth via the inactivation of Id-1/NF-κB signaling axis. Int J Oncol. 2016;49(5):1953–62.

28. Zhou Z, Zhou H, Zou X, Wang X, Yan M. Formononetin regulates endothelial nitric oxide synthase to protect vascular endothelium in deep vein thrombosis rats. Int J Immunopathol Pharmacol. 2022;36:3946320221111117.

29. Ou M, Zhang Y, Cui S, Zhao S, Tu J. Upregulated MiR-9-5p Protects Against Inflammatory Response in Rats with Deep Vein Thrombosis via Inhibition of NF-κB p50. Inflammation. 2019;42(6):1925–38.

30. Livak KJ, Schmittgen TD. Analysis of relative gene expression data using real-time quantitative PCR and the 2(-Delta Delta C(T)) Method. Methods (San Diego, Calif). 2001;25(4):402–8.

31. Zhang Z, Hu L, Chen W, Zhou C, Gui G, Lin B. Danhong huayu koufuye prevents deep vein thrombosis through anti-inflammation in rats. J Surg Res. 2016;201(2):340–7.

32. Wang Z, Ni S, Zhang H, Fan Y, Xia L, Li N. Silencing SGK1 alleviates osteoarthritis through epigenetic regulation of CREB1 and ABCA1 expression. Life Sci. 2021;268:118733.

33. Liu J, He Q. Ca(2+)/calmodulin-dependent protein kinase IV attenuates inflammation and mitochondrial dysfunction under insulin resistance in C2C12 cells. Arch Physiol Biochem 2020;1–10

34. Li K, Yang J, Lei XF, Li SL, Yang HL, Xu CQ, et al. EZH2 inhibition promotes ANGPTL4/CREB1 to suppress the progression of ulcerative colitis. Life Sci. 2020;250:117553.

35. Chen J, Ding Q, Jiao X, Wang B, Sun Z, Zhang Y, et al. Dexmedetomidine attenuates hippocampal neuroinflammation in postoperative neurocognitive disorders by inhibiting microRNA-329-3p and activating the CREB1/IL1RA axis. Psychopharmacology. 2022;239(7):2171–86.

36. Bombeli T, Karsan A, Tait JF, Harlan JM. Apoptotic vascular endothelial cells become procoagulant. Blood. 1997;89(7):2429–42.

37. Matsuzaki S, Pouly JL, Canis M. Effects of U0126 and MK2206 on cell growth and re-growth of endometriotic stromal cells grown on substrates of varying stiffness. Sci Rep. 2017;7:42939.

38. Santulli P, Marcellin L, Chouzenoux S, Boulard V, Just PA, Nicco C, et al. Role of the protein kinase BRAF in the pathogenesis of endometriosis. Expert Opin Ther Targets. 2016;20(8):1017–29.

39. Feng Y, Tan BZ. LncRNA MALAT1 inhibits apoptosis of endometrial stromal cells through miR-126-5p-CREB1 axis by activating PI3K-AKT pathway. Mol Cell Biochem. 2020;475(1–2):185–94.

40. Yang J, Liu S, Wang H, Liu Y, Liu Y. miR-134-5p inhibition reduces infarct-induced cardiomyocyte apoptosis via Creb1 upregulation. J Stroke Cerebrovasc Dis : the official journal of National Stroke Association. 2020;29(8):104850.

41. Zhang T, Ge J. Mechanism of CREB1 in cardiac function of rats with heart failure via regulating the microRNA-376a-3p/TRAF6 axis. Mammalian Genome : official journal of the International Mammalian Genome Society. 2022;33(3):490–501.

42. Hassan FM, Alsultan A, Alzehrani F, Albuali W, Bubshait D, Abass E, et al. Genetic Variants of RPL5 and RPL9 Genes among

Saudi Patients Diagnosed with Thrombosis. Med Arch (Sarajevo, Bosnia and Herzegovina). 2021;75(3):188–93.

43. Wang G, Zhao W, Yang Y, Yang G, Wei Z, Guo J. Identification of biomarkers of venous thromboembolism by bioinformatics analyses. Medicine. 2018;97(14):e0152.

44. Watanabe M, Toyomura T, Wake H, Nishinaka T, Hatipoglu OF, Takahashi H, et al. Identification of ribosomal protein L9 as a novel regulator of proinflammatory damage-associated molecular pattern molecules. Mol Biol Rep. 2022;49(4):2831–8.

45. Huang T, Jiang C, Yang M, Xiao H, Huang X, Wu L, et al. Salmonella enterica serovar Typhimurium inhibits the innate immune response and promotes apoptosis in a ribosomal/TRP53-dependent manner in swine neutrophils. Vet Res. 2020;51(1):105.

46. Iosef C, Alastalo TP, Hou Y, Chen C, Adams ES, Lyu SC, et al. Inhibiting NF-κB in the developing lung disrupts angiogenesis and alveolarization. Am J Physiol Lung Cell Mol Physiol. 2012;302(10):L1023–36.

47. Ma J, Li X, Wang Y, Yang Z, Luo J. Rivaroxaban attenuates thrombosis by targeting the NF-κB signaling pathway in a rat model of deep venous thrombus. Int J Mol Med. 2017;40(6):1869–80.

48. Lu Z, Ye Y, Liu Y, Yang X, Ding Q, Wang Y, et al. Aqueous extract of Paeoniae Radix Rubra prevents deep vein thrombosis by ameliorating inflammation through inhibiting GSK3β activity. Phytomed : international journal of phytotherapy and phytopharmacology. 2021;92:153767.